

Effect of nonlinear wave–particle interaction on electron-cyclotron absorption

C Tsironis and L Vlahos

Department of Physics, Aristotle University of Thessaloniki, 54124 Thessaloniki, Greece

Received 16 November 2005, in final form 26 June 2006

Published 1 August 2006

Online at stacks.iop.org/PPCF/48/1297

E-mail: ctsironis@astro.auth.gr

Abstract

We perform a self-consistent analysis of the nonlinear interaction of magnetized plasmas with electron-cyclotron (EC) waves. A closed set of equations is derived, which consists of the relativistic equations of motion under the wave field and the wave equation for the vector potential. The plasma is described in terms of ensembles of electrons which collectively determine the evolution of the wave amplitude and frequency through the current response. This description allows for effects of the electron motions on the efficiency of the wave absorption, for example, the asynchrony between the wave phase and the gyroperiod. As an application, we study the absorption of an EC wave beam in a simplified tokamak geometry, for plasma parameters relevant to current and future fusion experiments. We conclude that, within the limits of our model, there are cases where the linear theory for the absorption of EC waves, used widely in the current literature, may overestimate the energy deposition. In such cases, nonlinear effects are essential for the accurate estimation of the plasma-wave coupling and their inclusion should be considered, especially when the wave power is dramatically increased as in the case of ITER.

1. Introduction

The injection of electron-cyclotron (EC) waves is nowadays a well-established method for coupling energy to plasma electrons in modern fusion devices, with primary applications the plasma heating (ECRH) and the generation of non-inductive current drive (ECCD) [1–3]. At the same time, ECRH and ECCD have shown their importance in tokamak studies and their present usage goes beyond their heating and current drive application. In current fusion experiments, the EC radiation is launched in the plasma in the form of spatially narrow wave beams, and the plasma electrons interact with the wave when the EC resonance condition is realized:

$$\omega - k_{\parallel} v_{\parallel} - \frac{n\omega_c}{\gamma} = 0 \quad (n = 0, \pm 1, \pm 2, \dots), \quad (1)$$

where ω , ω_c are the wave and the nonrelativistic cyclotron frequency, k_{\parallel} , v_{\parallel} are the components of the wavenumber and the electron velocity parallel to the main magnetic field and γ is the relativistic Lorentz factor. Since the cyclotron frequency is proportional to the magnetic field, which is non-uniform in fusion devices, this condition is satisfied in a narrow spatial region. The suppression of the neoclassical tearing mode (NTM) and sawtooth activity and the formation of internal transport barriers (ITB) are examples of employing the advantage of EC waves to allow well-localized power deposition (see [1] and references therein).

ECRH studies are formally split in the experiments involving the injection of EC waves on the one hand, and on the other in the theoretical investigations related to the propagation and absorption of the radiation. With respect to the theory, it is very important to have a quantitative model for the way the wave propagates and is absorbed inside the plasma, as well as for the effects the resonant electrons have on the wave. In this sense, the ECRH theoretical studies may be divided into two different parts: the problem of wave propagation and absorption in the plasma, which studies the effect of the plasma on the wave, and the problem of the evolution of the resonant electron distribution function, which involves the effect of the wave on the plasma. One usually treats each part of the problem separately, where a coupling of the two parts constitutes the core of a self-consistent treatment. Due to the complex dependence of the power deposition on various factors, i.e. the magnetic field, the geometry of the beam and the plasma response, a realistic study of such problems requires a numerical treatment.

The propagation of EC waves inside the plasma is described by the solution of Maxwell equations. When the wavelength is small compared with the scale length of inhomogeneity of the medium (short-wavelength limit), which is mostly the case in modern ECRH experiments, a simplification is reached by using asymptotic methods, i.e. ray tracing [4], the complex eikonal method [5, 6] or beam tracing [7]. The solution is obtained with the use of the Hamiltonian differential equations, in some cases even ordinary ones [4, 7], where the dispersion function plays the role of the Hamiltonian. Such treatments provide a very direct physical picture of the process in terms of Hamiltonian rays. In most applications, the cold plasma dispersion function [8] is used as the Hamiltonian function. This choice is justified by the fact that, apart from the very narrow region of resonant interaction, the wave-plasma interaction is very weak. However, the direction of ray propagation can differ dramatically if the hot plasma dielectric tensor is used instead of the cold one for describing the wave propagation [9]. This implies effects on the evolution of the polarization vector, especially near the resonance, and thus on the absorption of the wave.

In solving Maxwell equations, one needs to know the current density induced by the wave field. In the majority of fusion applications, this quantity is derived in terms of the linear theory of plasma oscillations [10, 11]. The current density is calculated as the first-order moment of the electron distribution function, which comes as a solution of the linearized Vlassov equation assuming a Maxwellian unperturbed distribution. The current density, which contains all the information about the absorption of the EC wave in the inhomogeneous plasma, is finally expressed in terms of the dielectric tensor of a homogeneous, uniformly magnetized plasma, a form very suitable for applications. Such a simplified treatment is supported by the consideration that, for parameters relevant to modern experiments, the wave intensity is small and falls in the linear regime.

Regarding the plasma response to ECRH, the analysis developed so far is quite different from the linear approach. The state of the art is based on the assumption that the background electron distribution does not stay close to the Maxwellian distribution. The evolution of the distribution function is mainly being considered in the framework of the quasilinear approximation, where the effect of the resonant wave-particle interaction on the unperturbed

distribution is analysed in the case of small-amplitude plasma oscillations [12–14]. The unperturbed distribution function is found to obey a Fokker–Planck diffusion equation [14], where the effect of the resonant particles is described by diffusion coefficients quadratic in the wave amplitude. This additional diffusion may destroy the balance in the velocity space sustained by the particle collisions and creates the possibility for the formation of plateau regions in the distribution.

There are several ray and beam tracing codes that implement the linear theory for EC wave absorption [15, 16], and the results obtained are in agreement with a number of transmission experiments from different tokamaks [1–3]. Also, the quasilinear theory for the distribution function is the core of sophisticated Fokker–Planck codes [17, 18], which model the velocity space more accurately and agree with certain experimental results, i.e. the increase of ECCD efficiency due to suprathermal electrons (see for example [1]). It is widely believed that nonlinear effects are to play an important role only in cases when the injected power is very large, e.g. using a free-electron-laser (FEL) instead of gyrotrons as an ECRH source. FEL offers the possibility of high-power radiation over a wide range of frequencies with good efficiencies [19, 20]. In such cases, a reduction in the absorption appears due to nonlinear effects, which tend to prevent electrons from satisfying the condition (1) during the wave-particle interaction [21–23].

However, recent developments in theory and experiments imply that nonlinear effects already appear at lower values of the wave power. In [24, 25], a nonlinear kinetic modelling of ECRH and ECCD was performed, and the results show that the deviation from the linear and quasilinear theories can be significant for present day experiments. In experimental results from the W7-AS stellarator, disagreement with the predictions of linear modelling is observed for intense ECRH beams [26]. A possible source of the disagreement may be related with the fact that the ratio of the particle transit time through the beam and the characteristic time of trapped (in the wave) oscillations, takes values well into the nonlinear regime for parameters relevant to modern experiments. In such cases, the linear and quasilinear theories cease to provide a valid description. The problem of the nonlinear interaction of charged particles with plane electromagnetic waves has a long history (see [27–29] and references therein). Several authors used the quasilinear theory for the modelling of the electron distribution function and analysed the limits of its validity [30–32].

All the above studies show that the role of nonlinear effects in ECRH and ECCD is still an open issue. The understanding of the basic ECRH physics appears to be concise and able to describe the heating process; however this confidence is probably based more on the global success of past ECRH experiments than on the detailed agreement between theoretical predictions and experimental measurements. At the same time, the self-consistent treatment of ECRH scenarios is a very challenging problem and very crucial for the improvement of the modelling, which so far remains unexplored.

In this work, we present a self-consistent analysis of EC wave energy coupling to plasmas, the plasma being described in terms of ensembles of electrons moving under the wave field. We use the term ‘self-consistent’ in the sense that the electron motions, in their fully relativistic form, are followed and then drive the temporal evolution of the wave amplitude and the frequency through the current density term in the wave equation. In this description, effects of the particle motions on the efficiency of the wave absorption, for example, the loss of synchronism between the wave phase and the gyroperiod (which is connected to the role of anomalous diffusion in wave-particle interaction, see for example [32] and references therein) are fully taken into account. As an application, we study the absorption of an EC beam in a localized region with dimensions comparable to the characteristic scales of the inhomogeneity of the plasma profiles, a geometry allowing for simplifications in the numerical modelling.

We present results for plasma and wave parameters relevant to the ASDEX Upgrade (AUG) experiment and to ITER scenarios.

2. Self-consistent model for nonlinear wave-particle interaction

In the following, we describe a nonlinear and self-consistent model for wave-particle interaction. The modelling relies on the coupling of the relativistic equations of motion under the wave field with the wave equation in the presence of the plasma electrons. This set of equations provides a complete description of the dynamics of charged particles interacting with electromagnetic fields. The particle orbits are used to calculate the appropriate driving currents for the electromagnetic field, and the response current densities are, in turn, used to derive a system of equations describing the temporal evolution of the wave amplitude and frequency.

In this model, the electromagnetic wave (ω, \mathbf{k}) propagates in the xz plane at an angle θ with respect to the uniform magnetic field of the plasma $\mathbf{B} = B_0 \mathbf{z}$. The wave field is described by the vector potential

$$\mathbf{A} = A_0(t)[\pi_x \cos \theta \sin \phi(t) \hat{\mathbf{x}} + \pi_y \cos \phi(t) \hat{\mathbf{y}} - \pi_z \sin \theta \sin \phi(t) \hat{\mathbf{z}}], \quad (2)$$

where $A_0(t) = [8cP(t)]^{1/2}/w\omega(t)$ is the vector potential amplitude, expressed in terms of the wave power $P(t)$, with w the spatial width of the wave field and c the speed of light in vacuum, π_x, π_y and π_z are integers that determine the polarization of the wave and $\phi(t)$ is the wave phase [33]

$$\phi(t) = k(x \sin \theta + z \cos \theta) - \int_0^t \omega(t') dt', \quad (3)$$

where k is the wavenumber for the specific polarization. The integral on the right-hand side of equation (3) occurs from the integration of the relation $d\phi/dt = \mathbf{k} \cdot \mathbf{v} - \omega$ for the time-derivative of the wave phase. In this self-consistent description of wave-particle interaction, in the sense explained above, any effects due to wave-particle coupling are reflected in this temporal evolution.

Using the gauge $\Phi = 0$ and taking also into account that $\nabla(\nabla \cdot \mathbf{A}) = 0$ (for the specific form (2)), the equations of electron motion under the electromagnetic wave are

$$\begin{aligned} \frac{d\mathbf{r}}{dt} &= \frac{\mathbf{p}}{\gamma m_e c} \\ \frac{d\mathbf{p}}{dt} &= \frac{\omega_c}{\gamma} \mathbf{z} \times \mathbf{p} - \frac{e}{c} \left[\frac{\partial \mathbf{A}}{\partial t} + \frac{\mathbf{p} \times (\nabla \times \mathbf{A})}{\gamma m_e} \right], \\ \frac{d\gamma}{dt} &= -\frac{e}{\gamma m_e^2 c^3} \mathbf{p} \cdot \frac{\partial \mathbf{A}}{\partial t} \end{aligned} \quad (4)$$

where e and m_e are the electron charge and rest mass respectively, $\omega_c = eB_0/m_e c$ is the cyclotron frequency and \mathbf{p} is the relativistic mechanical momentum. In the equation involving $d\mathbf{p}/dt$, the first term on the right-hand side is the Lorentz force owing to the background magnetic field $B_0 \mathbf{z}$. The wave equation for the vector potential is

$$\nabla^2 \mathbf{A} - \frac{1}{c^2} \frac{d^2 \mathbf{A}}{dt^2} = -\frac{4\pi}{c} \mathbf{j}, \quad (5)$$

with \mathbf{j} the response electron current density. Replacing the expression (2) for \mathbf{A} in the wave equation (5) and performing a trigonometric elimination, one obtains equations describing the temporal evolution of A_0 and ω :

$$\begin{aligned} \frac{d^2 A_0}{dt^2} + A_0(c^2 k^2 - \omega^2) &= 4\pi c(j_x \cos \theta \sin \phi + j_y \cos \phi - j_z \sin \theta \sin \phi) \\ A_0 \frac{d\omega}{dt} + 2\omega \frac{dA_0}{dt} &= 4\pi c(-j_x \cos \theta \cos \phi + j_y \sin \phi + j_z \sin \theta \cos \phi) \end{aligned} \quad (6)$$

In the relations (6), as given above, A_0 , ω have an explicit dependence only on time, while the right-hand sides depend also on the particle positions through the wave phase and the current density. For cases where the dimensions of the region under study are small compared with the characteristic scales of spatial variation (e.g. magnetic field and density profile), and since the wave phase is periodic over space with periods $2\pi/k_x$, $2\pi/k_z$, this is simplified by averaging (6) over space. Thus, from here on, in considering (6) the right-hand side terms are replaced with their mean values over space.

Assuming an initial electron distribution function $f_0(\mathbf{r}_0, \mathbf{p}_0)$, the electron current density in the plasma has the form

$$\mathbf{j}(\mathbf{r}, t) = -\frac{en_e}{\gamma m_e} \int d^3\mathbf{r}_0 d^3\mathbf{p}_0 f_0 \mathbf{p} \delta[\mathbf{r} - \tilde{\mathbf{r}}(\mathbf{r}_0, \mathbf{p}_0, t)], \quad (7)$$

with $\tilde{\mathbf{r}}(\mathbf{r}_0, \mathbf{p}_0, t)$ the position at time t of the particle with initial conditions $\mathbf{r}_0, \mathbf{p}_0$. The existence of the delta function in the above equation indicates that contributions to the current density come only from particles of the initial distribution. In applications, where the number of particles constituting the electron distribution is finite, the integral in equation (7) (or any similar integral) is calculated as a sum on these particles. Assuming that the initial electron distribution is spatially-homogeneous, and taking into account the form of the current density, equations (6) become

$$\begin{aligned} \frac{d^2 A_0}{dt^2} + A_0(c^2 k^2 - \omega^2) \\ = \frac{c\omega_p^2}{e} \int d p_{0x} d p_{0y} d p_{0z} f_0 \left\langle \frac{p_z \sin \theta \sin \phi - p_x \cos \theta \sin \phi - p_y \cos \phi}{\gamma} \right\rangle \quad (8) \\ A_0 \frac{d\omega}{dt} + 2\omega \frac{dA_0}{dt} = \frac{c\omega_p^2}{e} \int d p_{0x} d p_{0y} d p_{0z} f_0 \left\langle \frac{p_x \cos \theta \cos \phi - p_y \sin \phi - p_z \sin \theta \cos \phi}{\gamma} \right\rangle, \end{aligned}$$

where $\omega_p^2 = 4\pi e^2 n_e / m_e$ is the plasma frequency, n_e being the electron plasma density, and the mean values indicated are over space. Equations (4) and (8) constitute a closed, self-consistent set describing the wave-plasma system, where the amplitude A_0 and the frequency ω in (4) are calculated as solutions of (8), while the integrals involved in (8) are determined from the solutions of (4) for the electron orbits.

The model presented above is general, in the sense that it contains all the physics of the interaction of electromagnetic waves with electrons. Thus, it can be met in a wide variety of relevant applications, like particle acceleration in the ionosphere and beam-plasma instabilities. Similar approaches have been followed in [33, 34] for the study of the EC maser mechanism, with applications to high-frequency radiation production [33] and the interpretation of solar microwave spikes [34] and also in [23] for the nonlinear absorption of ordinary waves with a frequency close to the cyclotron frequency. In this paper, the application lies in the field of plasma heating and considers the absorption of finite wave beams in the EC frequency regime.

3. EC absorption in tokamak plasmas

We apply the model described above to the study of EC beam absorption in a tokamak, considering a simplified plasma geometry and a finite region of wave-particle interaction (slab), which is visualized in figure 1. In the directions perpendicular to the beam propagation, the slab is defined by the projection of the beam width onto the magnetic axis, while along the propagation the slab width corresponds to a 2% relative variation of the toroidal field,

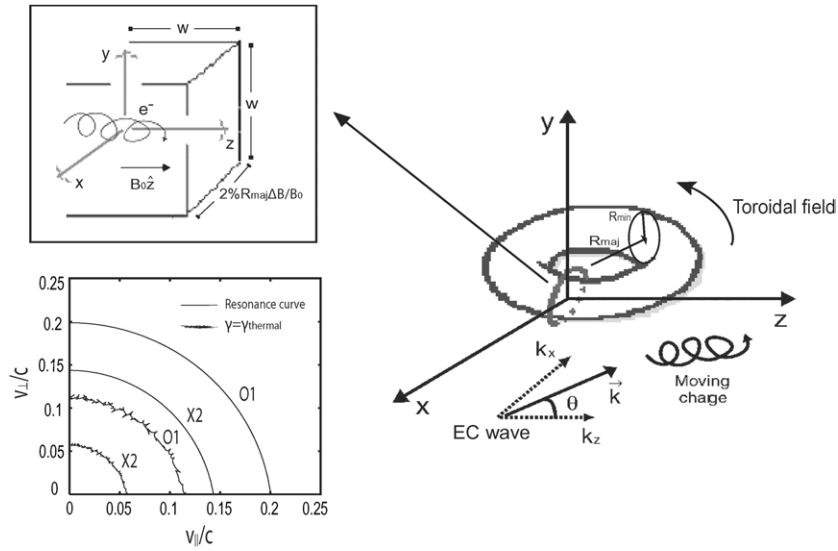


Figure 1. The plasma and magnetic field geometry: the upper figure shows a magnification of the finite region of wave-particle interaction; the lower one shows, in the velocity space, the resonance curve and the curve defined by the thermal velocity for the cases of perpendicular 2nd harmonic X-mode and 1st harmonic O-mode.

assuming a profile $B_0(1 + x/R_{maj})^{-1}$ with R_{maj} being the major tokamak radius. Under this choice, the dimensions of the slab are small compared with the characteristic length of variation not only of B_0 , but also of n_e and T_e , assuming typical parabolic profiles $\sim 1 - (x/R_{min})^2$, R_{min} being the minor tokamak radius and for values of the aspect ratio R_{max}/R_{min} relevant to modern tokamaks. Thus, these parameters may be assumed constant in the slab region, and as a consequence the wavenumber and the beam width are also constant. The plasma particles are initialized within the slab region and interact with the wave while inside the slab. After a particle exits the slab, its contribution to the current density of the plasma is not taken into account.

In order to have a meaningful comparison with the mainstream of applications of the linear theory for absorption, which correspond to a plasma that is stationary, inhomogeneous and collisionless, proper choices must be made for the modelling time and the calculation of linear absorption. In stationary models of plasma heating, the wave power is considered to be constant in time and varies in space within the layers of absorption. If P_0 is the ECRH power, then the power absorbed in the plasma is

$$\Delta P = P_0 \left[1 - \exp \left(- \int_0^{\Delta l} \alpha_L ds \right) \right], \quad (9)$$

where Δl is the length of the propagation path, α_L is the linear absorption coefficient and s the coordinate along the propagation. The energy absorbed by the plasma is $\Delta P \cdot \tau$, where τ is the heating time. It is obvious that in such models, at least for the evolution of the wave amplitude and power, time acts as an external parameter. In reverse, in our model the wave amplitude and frequency, and consequently the wave power, are constant in space within the regions under study but vary in time. The wave evolution is subject to temporal effects related to the propagation and particle motions. In order to reconcile the above, we trace the wave and the particles for the time t_{int} needed by the beam, moving with the maximum possible group velocity c , to cross the slab. This means that, in our comparisons, we consider only

the fraction of energy crossing the slab in this time-window and assume that the behaviour traced within this window is repeated as the wave energy comes continuously from the source towards the slab. This characteristic time is much smaller than the collision time, so collision effects can safely be neglected. The ratio P/P_0 is followed using nonlinear equations (4) and (8) and compared with ratio (9) coming from the linear theory, where $\int_0^{\Delta l} \alpha_L ds = \alpha_L \Delta l$ with Δl being the dimension of the slab along the propagation.

We perform simulations for parameters relevant to the AUG tokamak, as well as to the experiments planned for ITER. In both cases, the wavenumber is calculated as the solution of the cold plasma linear dispersion relation for the specific wave polarization, 2nd harmonic X-mode in AUG (for the indices appearing in (2) it is $\pi_x = \pi_y = \pi_z = 1$) and 1st harmonic O-mode in ITER ($\pi_x = \pi_z = 1, \pi_y = -1$). The linear absorption coefficient is evaluated on the basis of the wave-plasma energy balance, taking into account weakly relativistic and finite Larmor radius effects [35]. In our simulations for AUG, the major and minor radius of the tokamak is $R_{\text{maj}} = 165$ cm and $R_{\text{min}} = 60$ cm, respectively, the main magnetic field is $B_0 = 2.5$ T, the plasma density is $n_e = 10^{13}$ cm $^{-3}$ and the temperature is $T_e = 1$ KeV. At $t = 0$, the plasma follows a relativistic Maxwellian (Juettner) distribution:

$$f(\gamma)|_{t=0} = \frac{1}{\mu K_2(\mu^{-1})} \gamma(\gamma^2 - 1)^{1/2} \exp(-\mu\gamma), \quad (10)$$

where $\mu = m_e c^2 / T_e$ and $K_2(\mu^{-1})$ is the modified Bessel function of the second kind [36] with index 2 and argument μ^{-1} . The wave is injected at angles $\theta = 70^\circ$ (corresponding to a toroidal angle 20°) and 90° (perpendicular to the magnetic field) in the form of a square-shaped beam with half-width $w = 2$ cm. In all cases, the initial frequency of the wave is chosen such that it satisfies the resonance condition (1). In figure 1 we show the position of the resonance curve in velocity space, compared with the curve $\gamma = \gamma_{\text{th}}$ defined by the thermal velocity of the initial distribution for the case of perpendicular injection. The equations are numerically solved using a Runge–Kutta method of 4th order with step 10^{-2} (the use of methods with a variable step did not yield differences in the results).

In figure 2(a) we show the wave power, normalized over its initial value, for an oblique injection ($\theta = 70^\circ$). The power of the beam is $P_0 = 1$ MW and the initial frequency $\omega_0 = 1.98\omega_c$. The horizontal line appearing in the figure stands for the fraction of the remaining wave power, $P/P_0 = (P_0 - \Delta P)/P_0$, as predicted by linear theory. This quantity does not have any time-dependence and depends only on the length of the region of wave–particle interaction. The wave power is absorbed by the plasma particles with a rate moderately smaller from that predicted by the linear theory. In figure 2(b) the temporal evolution of the wave frequency, normalized to the cyclotron frequency, is plotted. One can see that the frequency oscillates around the initial value $\omega_0 \sim 2\omega_c$. A power spectrum analysis on the time-series of the values of ω showed that there are no dominant frequencies in the spectrum, which implies that these oscillations are of nonlinear nature, owing to the nonlinear character of the energy exchange between the wave and the particles. This behaviour, which appears also in the evolution of the amplitude (see again figure 2(a)), indicates that the effect of the electrons is not limited only in the loss of wave power but also in the characteristics of the wave emission in the plasma. In figure 2(c) the exit electron distribution function is compared to the initial distribution f_0 . The comparison was followed over very small regions of the energy space (see inset) and showed that the effect of the ECRH power on the electron distribution is small. This is because the time of wave–particle interaction in our simulations is very small with respect to the (quasilinear) time scale for the evolution of the distribution function, and thus the energy coupled to the particles is not enough to modify significantly the distribution. The energy exchange between the wave and the particles is visualized in figure 2(d), where the evolution of the mean kinetic

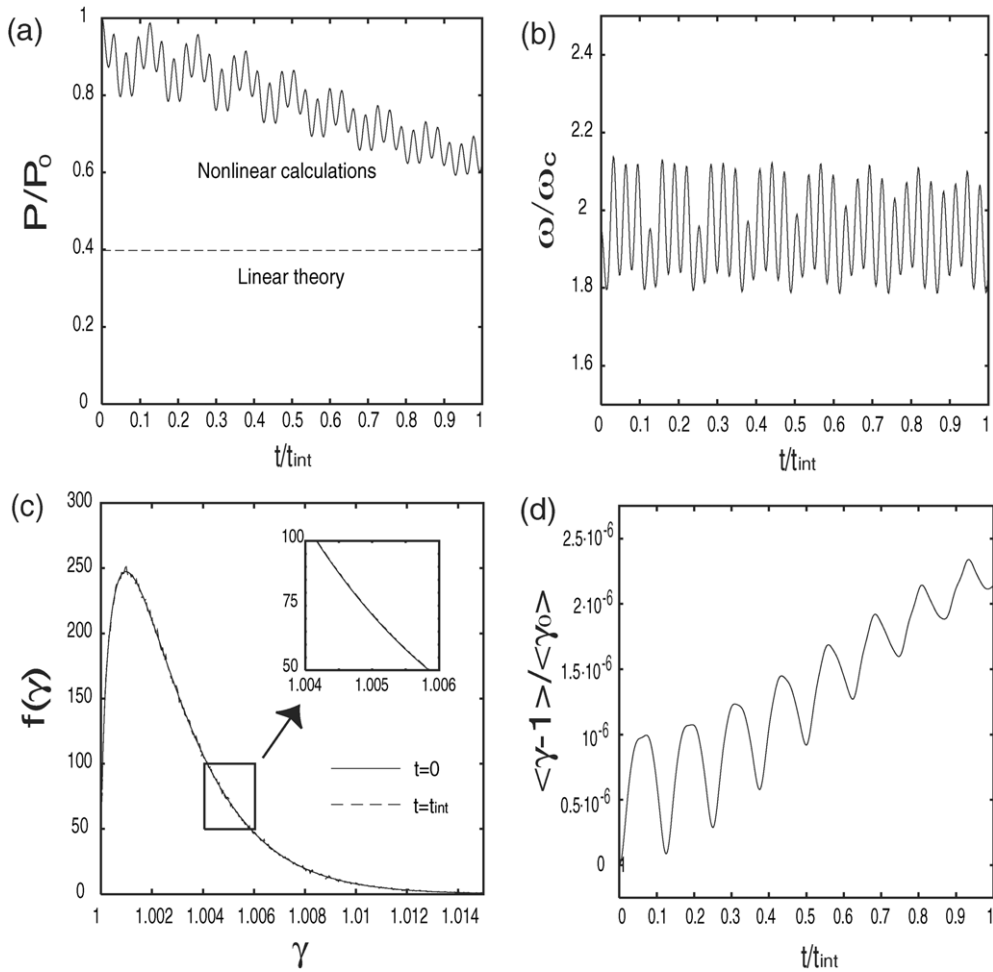


Figure 2. Simulation of ECRH for AUG parameters $P_0 = 1 \text{ MW}$, $\theta = 70^\circ$: (a) normalized wave power P/P_0 (from linear theory and nonlinear modelling) versus time, (b) normalized frequency ω/ω_c versus time, (c) distribution function $f(\gamma)$ at $t = 0$ and $t = t_{\text{int}}$ and (d) normalized mean electron kinetic energy $\langle \gamma - 1 \rangle / \langle \gamma_0 \rangle$ versus time.

energy $\langle \gamma - 1 \rangle$ (normalized to the total initial energy) is shown. The energy gain of the electrons due to absorption of the EC wave is obvious.

We continue our study with the case of perpendicular injection for the same wave power and initial frequency as above. In figure 3(a) we plot the temporal evolution of the normalized wave power. As in the previous case, the linear modelling appears to overestimate the rate of wave damping. Particularly in this case of perpendicular propagation, the nonlinear calculations show a significant reduction in the absorption. This is in accordance with recent results suggesting that the nonlinear effects during ECRH play a significant role in AUG experiments [24, 25]. In figure 3(b) the evolution of the plasma current across the propagation is shown. The increase in the perpendicular energy of the particles due to the wave-particle interaction is evident. The value of the current increases appearing oscillations similar to the ones of the cases examined above, due to the nonlinear character of the wave-particle energy exchange.

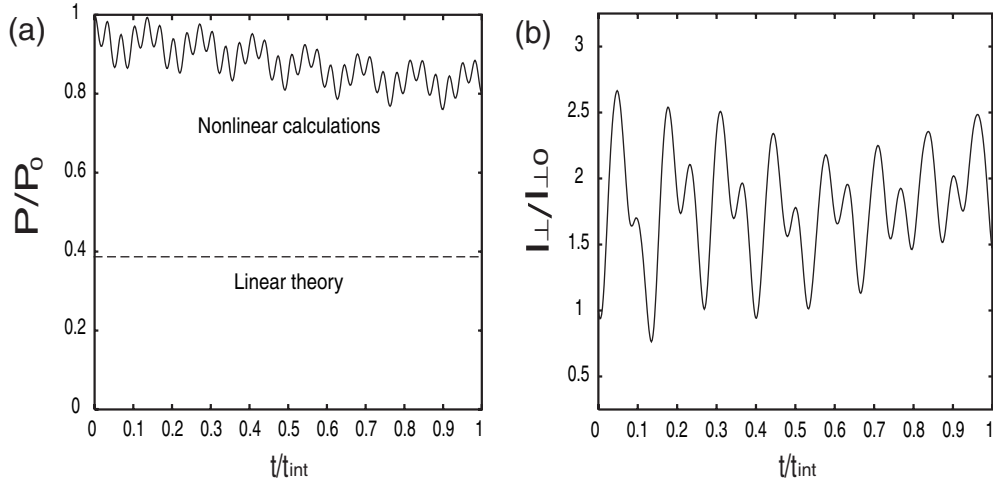


Figure 3. Simulation of ECRH for AUG parameters $P_0 = 1$ MW, $\theta = 90^\circ$ (perpendicular injection): (a) P/P_0 (from linear theory and nonlinear modelling) versus t/t_{int} and (b) current response across the magnetic field $I_\perp/I_{\perp 0}$ versus time.

We mentioned in the introduction that, as the wave power increases, the nonlinear effects become more intense due to the asynchrony between the wave phase and the gyroperiod. In order to emphasize this fact, we performed a simulation assuming the possibility of high ECRH-power injection, relevant to a FEL source, in AUG. The evolution of the wave power for the injection of a beam with $P_0 = 1$ GW ($\omega_0 = 1.98\omega_c$) at an angle $\theta = 70^\circ$ is shown in figure 4(a). In this case, because the energy coupled to the particles is very large and the temperature of the plasma in the region of simulation is increased importantly, we present also an additional type of result for the linear absorption that accounts for the temperature increase in the absorption coefficient. Specifically, the (approximate) thermal velocity of the electron distribution has been calculated numerically at each time instant and then used in the formula for α_L at this instant. The total power damped is given by (9), where the integral on the right-hand side is calculated as $\int_0^{\Delta l} \alpha_L ds = \langle \alpha_L \rangle \Delta l$, with $\langle \alpha_L \rangle$ the time-average of the absorption coefficient. The deviation from the linear absorption appears a little larger than in the case $\theta = 70^\circ$, $P_0 = 1$ MW treated above. In figure 4(b) the energy distribution function at $t = 0$ and $t = t_{\text{int}}$ is shown. The exit distribution differs significantly from its initial Maxwellian form, even though the time of wave–particle interaction is very small. In fact, the deviations that the distribution appears with respect to its Maxwellian best-fit, which is also shown in figure 4(b), imply that the exit distribution is not even Maxwellian. More specifically, a non-thermal tail appears due to the nonlinear character of the wave–particle interaction. There is a possibility this process could be described by quasilinear modelling, but in general the behaviour is highly nonlinear (see [30, 32] for examples); a more detailed modelling of the distribution function is beyond the scope of this work. The examination of both figures indicates that the role of nonlinear effects is very important both for the wave evolution and the plasma response.

We conclude this study with simulations which may be relevant to ITER. The major and minor radius of the tokamak is $R_{\text{maj}} = 620$ cm and $R_{\text{min}} = 190$ cm, respectively, while the magnetic field on the axis is $B_0 = 5.3$ T. The plasma electrons follow a relativistic Maxwellian distribution with density $n_e = 2 \cdot 10^{13}$ cm $^{-3}$ and temperature $T_e = 8$ KeV. We specifically treat the case where the EC wave is injected obliquely at an angle $\theta = 70^\circ$, in the form of a

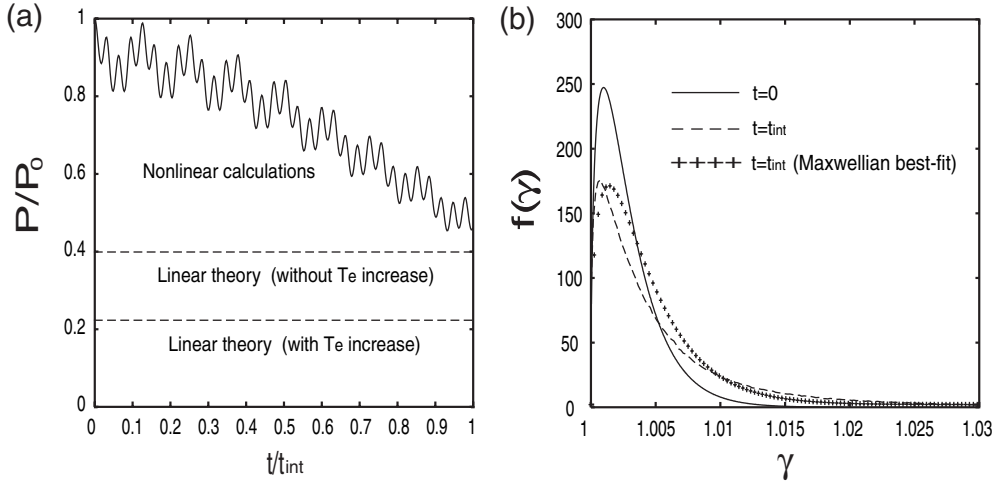


Figure 4. Simulation of ECRH for AUG parameters: (a) P/P_0 (from linear theory and nonlinear modelling) versus t/t_{int} and (b) $f(\gamma)$ versus γ at $t = 0$ and $t = t_{\text{int}}$, for injection ($\theta = 70^\circ$) of $P_0 = 1$ GW.

narrow beam with a square profile and half-width $w = 3$ cm. The beam power is $P_0 = 20$ MW and the initial frequency $\omega_0 = 0.98\omega_c$. In figure 5(a) we present the temporal evolution of the normalized wave power together with the linear result. The absorption appears more reduced than in the case of oblique ECRH in AUG treated above. This is in agreement with considerations based on the fact that, for ITER parameters, the ratio of the transit time through the beam and the characteristic time of trapped oscillations takes values even deeper into the nonlinear regime [25]. The nonlinear oscillations that characterize the behaviour of the system appear more rapid for this case. This is because the propagation path is larger and the plasma response is more intense for ITER parameters. In figure 5(b), the wave frequency as a function of t/t_{int} and the exit electron distribution function are plotted. The behaviour is similar to the case of AUG presented in figure 2.

The above results are consistent with the energy conservation, which in terms of the variation of the total wave-particle energy is written as $d(E_{\text{pl}} + E_{\text{wav}})/dV = 0$, where $dE_{\text{pl}}/dV = n_e \langle \gamma \rangle m_e c^2$ is the energy density of the plasma and $dE_{\text{wav}}/dV = A^2 \omega^2 / 4\pi c$ the energy density of the wave. Using these relations for the energy densities and normalizing, one obtains a simplified expression for the energy conservation

$$\omega_p^2 \Delta \langle \gamma \rangle + \Delta(A^2 \omega^2) = 0. \quad (11)$$

The consistency can be verified by numerically following the validity of (11) in the plasma volume occupied by the test particles. In figure 6(a) we present the temporal evolution of the left-hand side of equation (11), referred to as numerical error, for the set of parameters relevant to ITER. The accuracy is found to be of the order 10^{-6} . We should note that the numerical accuracy of the simulations depends strongly on the number of test particles used for the statistical description of the plasma, which in the simulations presented is $N \sim 10^6$. For the cases studied, increasing this number does not increase further the numerical accuracy. Further benchmarking of our model was performed with a comparison of the linear and nonlinear models for a very low value of the injected wave power, $P_0 = 10$ kW, for AUG parameters and oblique injection. The result is presented in figure 6(b), where the evolution of the wave power is shown, and the agreement between the two models is reasonable.

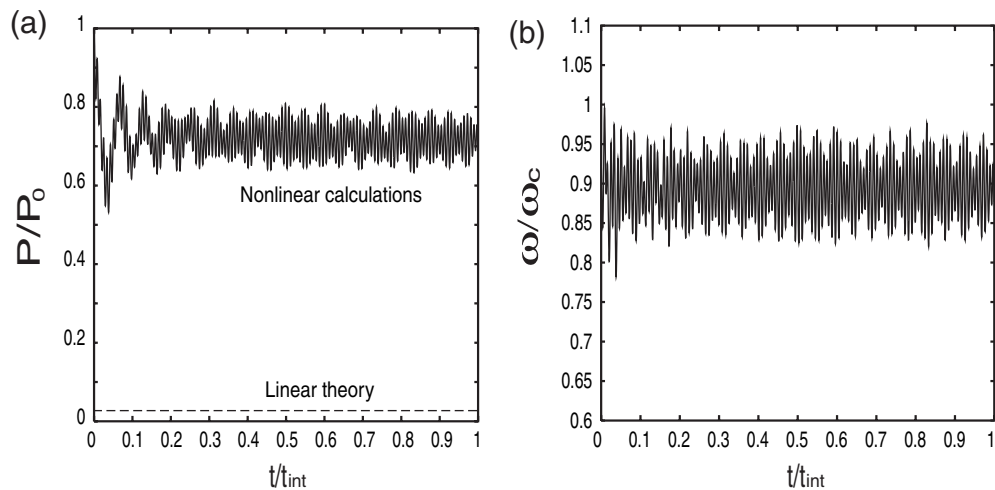


Figure 5. Simulation of ECRH for ITER parameters: (a) P/P_0 (from linear theory and nonlinear modelling) versus t/t_{int} and (b) ω/ω_c versus t/t_{int} .

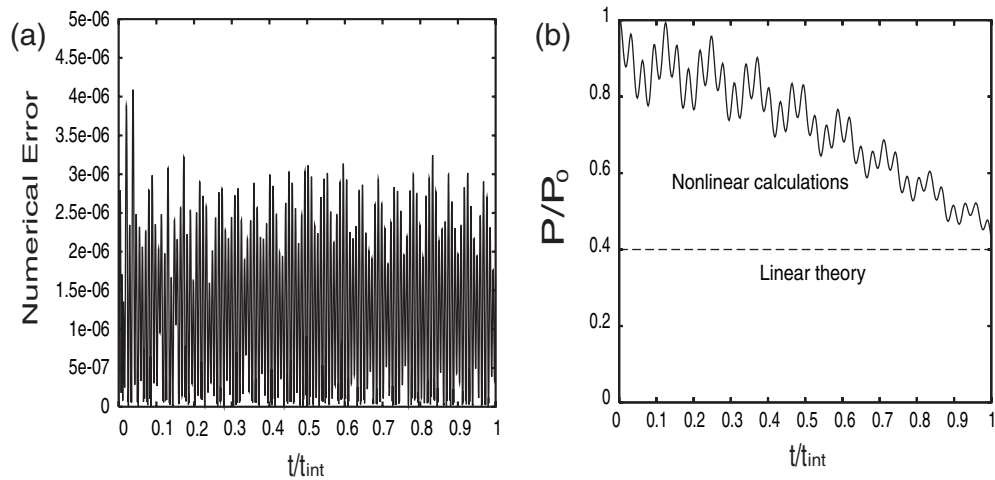


Figure 6. (a) Numerical error versus t/t_{int} for oblique injection of $P_0 = 20$ MW (ITER parameters), (b) P/P_0 (from linear theory and nonlinear modelling) versus t/t_{int} for oblique injection of $P_0 = 10$ kW (AUG parameters).

4. Summary and discussion

We have analysed in this paper the interaction of magnetized relativistic electrons with EC waves. A self-consistent model for wave–particle interaction has been developed, where effects of the particle motions on the evolution of the wave are accounted for. The model was applied for simulations of EC absorption for AUG and ITER experiments, considering a simplified geometry and a finite region for wave–particle interaction.

Our results are summarized as follows: for typical parameters relevant to current-day experiments, and within the limits of our model, the absorption of the EC wave appears reduced in comparison with the linear predictions. The reduction becomes more significant for propagation close to perpendicular. The effect on the electron distribution is little,

because the time of wave-particle interaction in our simulations is small compared with the time scale for the evolution of the distribution function. In the case of high ECRH-power sources (e.g. FELs), under the consideration of the temperature increase for this case, the deviation from linear theory appears more intense, as expected (see [20, 22]). Also, in this case the distribution presents a non-Maxwellian tail, even though the time of the wave-particle interaction is small. The wave frequency has a temporal variation of nonlinear nature, namely a nonlinear oscillation around its initial value. This indicates that the effect of the electrons is not limited only to the absorption but also in characteristics of the emission.

A discussion of the limitations to our model is essential. In general, the use of test particles in the description of physical problems has the cost of a large computational burden; simplifications and reduced scenarios are thus a necessity. Such considerations, which are also part of the literature cited in this paper, make the dependence of the wave parameters on both space and time to be more easily applied in practice, especially if numerical calculations are not a part of the study. Our viewpoint was to keep most of the physics in play and simplify the numerical computations by performing a local description of the wave-plasma interaction, in the sense that it does not take into account the spatial variation of the wave and plasma variables. In our description, we think of the global region of wave-particle interaction as a set of slices of small dimensions and study the physics of the wave-plasma system in such a local slice. From this viewpoint, the spatial dependence of the plasma parameters, i.e. the magnetic field, density and temperature profiles, may be neglected. This simplifies the numerical computations by omitting effects due to inhomogeneity of the plasma and magnetic field, such as the spatial variation of the wave-vector and the response current, ∇B particle drifts, etc.

In our statistical description of the plasma, we did not introduce particles entering the region of interaction during the simulation in order to reduce the computation time (when a particle exits the slab its motion is not further followed). Actually, the way the ensemble of particles is taken (polling) is a matter of choice, and the results based on different ensembles should not be significantly different (our computations also suggest this). We should note, of course, that the existence of particles exiting the volume during the computation does not affect the accuracy of the results, because this number of ‘lost particles’ is very small (maximum of 5% of the total ensemble).

The numerical accuracy and stability of our simulations depends strongly on the number of test particles used for the statistical description of the plasma. This is due to the fact that the terms on the right-hand side of equation (8) are very sensitive on the choice of N . Particularly in cases where the contribution of these terms is very large, e.g. when the plasma density is very high, the numerical procedure tends to become unstable because any statistical fluctuation in the calculation of the averages involved in (8) is of large order. At the moment, this disadvantage can be faced by increasing significantly the number of particles and reducing the time step, which makes the computational time extremely large. However, the model is still applicable considering the computer power and the parallelization methods available nowadays. An improved version of our model that accounts for issues such as the reduction of the importance of nonlinear effects as the plasma density increases (see e.g. [24]) will be attempted in further works.

As a closing remark, we believe that the understanding of the basic ECRH physics appears to be concisely describing the heating process; however this confidence is mainly based more on the global success of past ECRH experiments than on the detailed agreement between theoretical modelling and experiments, which has not yet been fully tested. In fact, it is extremely difficult to measure processes that take place in the very small plasma volume near

the resonance where the wave power is deposited. However, recent developments in theory and experiment suggest that nonlinear physics is present in current day fusion experiments. A proper treatment of ECRH and ECCD should probably be based on taking into account the nonlinear character of the wave-particle interaction. At the same time, the self-consistent feedback of the electron distribution on the wave beam may also be considered, in order to provide more accurate results. Our modelling is in this direction, however due to the simplifications the results are just indicative. The treatment of problems in ECRH/ECCD of practical interest, such as the suppression of MHD instabilities by applied ECRH or the modelling of ECCD in real magnetic geometry and topology with island structures and rational surfaces, require more sophisticated treatment taking into account the maximum extent of the physics involved in realistic geometry.

Acknowledgments

The authors would like to thank Drs H Isliker and I Sandberg for their comments on this paper. This work has been sponsored by the European Fusion Programme (Association EURATOM-Hellenic Republic) and the General Secretariat of Research and Technology. The sponsors do not bear any responsibility for the content of this work.

References

- [1] Erckmann V and Gasparino U 1994 *Plasma Phys. Control. Fusion* **36** 1869
- [2] Lloyd B 1998 *Plasma Phys. Control. Fusion* **40** A119
- [3] Prater R 2004 *Phys. Plasmas* **11** 2349
- [4] Bernstein I B 1975 *Phys. Fluids* **18** 320
- [5] Bravo-Ortega A and Glasser A H 1991 *Phys. Fluids B* **3** 529
- [6] Nowak S and Orefice A 1993 *Phys. Fluids B* **5** 1945
- [7] Pereverzev G V 1998 *Phys. Plasmas* **5** 3529
- [8] Stix T 1962 *The Theory of Plasma Waves* (New York: McGraw-Hill)
- [9] Westerhof E 1997 *Plasma Phys. Control. Fusion* **39** 1015
- [10] Bornatici M *et al* 1983 *Nucl. Fusion* **23** 1153
- [11] Swanson D G 1989 *Plasma Waves* (New York: Academic)
- [12] Suvorov E V and Tokman M D 1983 *Plasma Phys.* **25** 723
- [13] Timofeev A V and Tokman M D 1994 *Plasma Phys. Rep.* **20** 336
- [14] Brambilla M 1998 *Kinetic Theory of Plasma Waves* (New York: Oxford University Press)
- [15] Westerhof E 1980 *Rijnhuizen Report* **89-183**
- [16] Poli E *et al* 2001 *Comput. Phys. Commun.* **136** 90
- [17] Harvey R W 1992 *GA Report* **A20978**
- [18] Krivenski V 2001 *Fusion Eng. Des.* **53** 23
- [19] Robertson C W and Sprangle P 1989 *Phys. Fluids B* **1** 3
- [20] Cohen B I *et al* 1991 *Rev. Mod. Phys.* **63** 949
- [21] Nevins W M *et al* 1989 *Phys. Rev. Lett.* **59** 60
- [22] Allen S L *et al* 1994 *Phys. Rev. Lett.* **72** 1348
- [23] Kotelnikov I A and Stupakov G V 1990 *Phys. Fluids B* **2** 881
- [24] Kamendje R *et al* 2003 *Phys. Plasmas* **10** 75
- [25] Kamendje R *et al* 2005 *Phys. Plasmas* **12** 012502
- [26] Laqua H P *et al* 2004 *Proc. 31st EPS Conf. vol 28G (ECA)* 1.209
- [27] Roberts C S and Buchsbaum S J 1964 *Phys. Rev.* **135** A381
- [28] Menyuk C R *et al* 1988 *Phys. Fluids* **31** 3768
- [29] Polymilis C and Hizanidis K 1993 *Phys. Rev. E* **47** 4381
- [30] Hizanidis K *et al* 1989 *Phys. Fluids B* **1** 3 682
- [31] Farina D *et al* 1993 *Phys. Fluids B* **5** 104
- [32] Tsironis C and Vlahos L 2005 *Plasma Phys. Control. Fusion* **47** 131
- [33] Sprangle P and Vlahos L 1986 *Phys. Rev. A* **33** 1261

-
- [34] Vlahos L and Sprangle P 1987 *Astrophys. J.* **322** 463
[35] Bornatici M 1982 *Plasma Phys.* **24** 629
[36] Dennery P and Krzywicki A 1995 *Mathematics for Physicists* (New York: Dover)